

Capillary wrinkling of elastic membranes

D. Vella^{1,2}, M. Adda-Bedia², E. Cerda³

¹*ITG, Department of Applied Mathematics and Theoretical Physics,
University of Cambridge, Wilberforce Road, Cambridge, CB3 0WA, UK*

²*Laboratoire de Physique Statistique, Ecole Normale Supérieure, UPMC Paris 06,
Université Paris Diderot, CNRS, 24 rue Lhomond, 75005 Paris, France*

³*Departamento de Física, Universidad de Santiago, Av. Ecuador 3493, Santiago, Chile*

We present a physically-based model for the deformation of a floating elastic membrane caused by the presence of a liquid drop. Starting from the equations of membrane theory modified to account for surface energies, we show that the presence of a liquid drop causes an azimuthal compression over a finite region. This explains the origin of the wrinkling of such membranes observed recently [J. Huang *et al.*, *Science* **317**, 650 2007] and suggests a single parameter that determines the extent of the wrinkled region. While experimental data supports the importance of this single parameter, our theory under-predicts the extent of the wrinkled region observed experimentally. We suggest that this discrepancy is likely to be due to the wrinkling observed here being far from threshold.

I. INTRODUCTION

The idea that the equilibrium contact angle of a liquid droplet on a surface can be determined by considering the horizontal balance of the three surface ‘tensions’ acting at the contact line dates back more than two centuries to Young¹. However, the question of how the vertical balance of these same three tensions can be achieved has received attention only relatively recently. It is clear that at some microscopic scale this balance can only be achieved by the deformation of the substrate on which the droplet sits. This deformation can easily be studied in the case of one sessile droplet placed on top of another². It is more usual, however, for a drop to be sitting on the surface of a solid. For the small deformations anticipated here we expect that the substrate might be modelled using linear elasticity theory. The case of a semi-infinite elastic solid was considered by Lester³. However, one might expect the importance of vertical deformations to become even more important when the elastic solid becomes very thin as in plates and membranes. Fortes⁴ studied these problems using intuitive force balance arguments to relate the elastic deformation at the contact line to the contact angle of the liquid. Shanahan⁵ subsequently derived these force balances from energy considerations.

In recent years, the interaction between elasticity and capillarity hinted at by the vertical force balance at a contact line has become an area of considerable interest and importance in its own right. ‘Elasto-capillarity’ encompasses the stiction that can damage MEMS devices^{6,7} as well as the clumping of the hairs in a paintbrush at a more macroscopic level^{8,9}. In many of these situations it is enough simply to understand why clumping/stiction happens and how it might be avoided. However, it has also become clear that the influence of surface tension on the elastic deformation of an object can be a useful tool to infer material parameters that might otherwise be inaccessible¹⁰. For example, the commonly observed tearing instability of an elastic sheet adhered to a rigid substrate can also be used to characterize the adhesion

energy¹¹.

A novel experiment combining both the fundamental and applied aspects of the interaction between surface tension and elasticity was presented by Huang *et al.*¹². In this experiment, a small liquid drop was placed onto an elastic membrane that is itself floating on a bath of the same liquid. Before the addition of the drop, the membrane is stretched by the surface tension of the liquid bath. Once the drop is added, the opposing tension due to the contact line of the drop, causes radial wrinkles (see figure 1a-b). These wrinkles appear to emanate from the contact line of the drop but only have a finite length, L_w , defined in figure 1a. By a suitable series of calibration experiments, Huang *et al.* were able to infer *both* the thickness, h , of the membrane and also its elastic modulus, E , from a single image, which gave measurements of the number of wrinkles and the size of the wrinkled region, L_w . Using scaling arguments from earlier work^{13,14}, the dependence of the number of wrinkles on E and h could then be determined. However, no theory was available for the extent of the wrinkled region, L_w . Experimentally, it was found that

$$\frac{L_w}{R} \approx 0.031 \left(\frac{Eh}{\gamma_{lv}} \right)^{1/2}, \quad (1)$$

where R is the radius of the drop and γ_{lv} is the surface tension coefficient of the liquid–gas interface. To date, this relationship remains purely empirical. In this paper we set out to provide a theoretical justification for this result.

We also note that this experimental system is of fundamental interest from the point of view of the elasticity of thin objects. Azimuthal wrinkling is common whenever a thin sheet is loaded at a point because this loading causes a ring of material at radial distance r to move to a ring of smaller radius. The excess length of the ring must then be accommodated by buckling out of the plane, i.e. wrinkling. Recent examples where instabilities based on this essentially geometrical consideration have been found include: the impact of fast projectiles

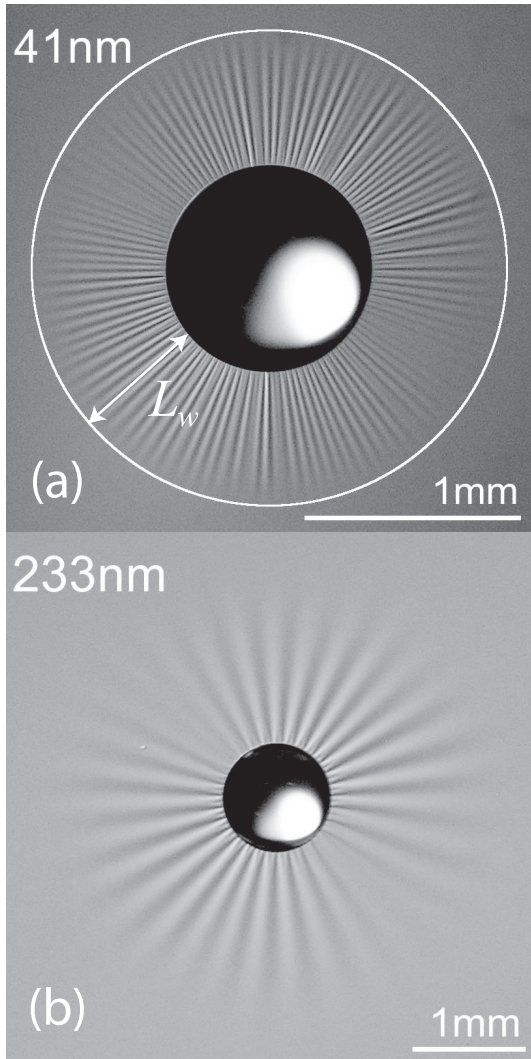


FIG. 1. Wrinkling of thin PS membranes floating on a liquid bath caused by liquid drops (taken from Huang *et al.*¹²). Two different membrane thicknesses (given in each figure) are shown here demonstrating that L_w depends on the thickness of the membrane, h . This paper is concerned with understanding the dependence of L_w on the system parameters.

onto free-falling membranes¹⁵, the scarring around circular wounds¹⁶ and the deadhesion of a thin sheet loaded at a point¹⁷. While all qualitatively similar, the details of the wrinkling pattern that forms depends on the details of the loading. This has been seen using thin floating membranes that are loaded using a ‘point-like’ load¹⁸. From these experiments it was found that a point-like load induces wrinkles throughout the domain. This is different from the case studied here (where wrinkling is localized) because of the different boundary conditions applied by the loading: a fixed tension at some radius in our case versus a fixed vertical displacement at $r = 0$ studied by Holmes & Crosby¹⁸. The experimental system of Huang *et al.*¹² with loading caused by a liquid drop is perhaps closest to the theoretician’s ideal because a

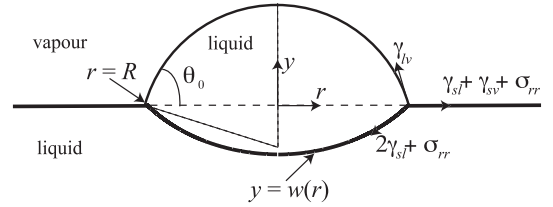


FIG. 2. Schematic showing a cross-section through an axisymmetric liquid drop sitting on an elastic membrane, which is itself floating on a bath of the same liquid (though the surface energy of the bath $\gamma'_{lv} \neq \gamma_{lv}$ in general due to the presence of surfactants). The radius of the circular contact line is R while the curvature of the drop is $\sin \theta_0 / R$ where θ_0 is the inclination of the interface to the horizontal.

known tension is applied at some radius.

II. IMPORTANT PHYSICAL PRINCIPLES

In this article we adopt a physically motivated approach to the problem of the deformation of a thin elastic membrane by a liquid drop. A more detailed mathematical derivation of the equations used to model this system can be found in the paper of Shanahan⁵. However, the application of these equations to the problem of wrinkling of a membrane is new.

We are primarily interested in determining the extent of the wrinkled region, which would usually¹⁹ be equivalent to the region in which there is an azimuthal compression, $\sigma_{\theta\theta} < 0$. We must therefore calculate the stress induced in a membrane by the presence of the drop and an underlying liquid. The situation is depicted in figure 2.

Although it is natural to account for the tension applied by the surface energy of the liquid drop, γ_{lv} , it is also important to account for the other surface energies, namely the solid–liquid surface energy, γ_{sl} , and the solid–vapour surface energy, γ_{sv} . The importance of including these additional energies arises because, when the membrane is stretched, the areas of the liquid–solid and solid–vapour interfaces increases also. Furthermore, the presence of these surface energies implies that the membrane is prestressed preventing buckling at compressive levels below the local pre-stress $\gamma(r)$, which is defined (see figure 2) as

$$\gamma(r) = \begin{cases} 2\gamma_{sl}, & r < R, \\ \gamma_{sl} + \gamma_{sv}, & r > R. \end{cases} \quad (2)$$

This is the physical basis for the mathematical model developed here. In this model we allow the liquid–vapour surface energy of the bath, γ'_{lv} , to differ from that of the drop, γ_{lv} . We shall present new experimental data incorporating this generalization in addition to the experimental data from the case $\gamma'_{lv} = \gamma_{lv}$ published previously¹².

III. A MATHEMATICAL MODEL

We begin by considering an axisymmetric membrane shape, $y = w(r)$, under some varying load, $q(r)$. We will also introduce the derivative of the Airy stress function ψ such that

$$\sigma_{rr} = \psi/r, \quad \text{and} \quad \sigma_{\theta\theta} = \frac{d\psi}{dr}. \quad (3)$$

(This is a standard step to ensure that the obtained deformation satisfies the equilibrium equations for the solid²⁰.) The large axisymmetric deformations of a plate caused by some loading $q(r)$ are described by the Föppl-von Kármán equation²⁰

$$B\nabla^2\nabla^2w - \frac{1}{r} \frac{d}{dr} \left(\psi \frac{dw}{dr} \right) = q(r), \quad (4)$$

where B is the bending stiffness of the plate. To ensure that the Airy stress function yields stresses (and hence strains) that are compatible with the deformation $w(r)$ we also require^{20,21}

$$r \frac{d}{dr} \left[\frac{1}{r} \frac{d}{dr} (r\psi) \right] = -\frac{1}{2} Eh \left[\frac{dw}{dr} \right]^2 \quad (5)$$

When large external stretching forces are applied to a thin plate it is possible to neglect the first term of (4), which represents bending, in comparison with the second term, which represents stretching. Since radial derivatives are of the order of the size of the water drop R and the stress in the membrane cannot be smaller than the surface tension γ_{lv} at the outer boundary, we may compare the relative sizes of the bending and stretching terms by calculating the value of the dimensionless parameter $B/(\gamma_{lv}R^2)$. For parameter values typical of the experiments of Huang *et al.*¹², this ratio is of the order 10^{-6} . In what follows, we therefore assume that stretching dominates bending and neglect the first term of (4). Before writing this ‘membrane equation’²⁰ we note that the presence of a pre-stress, $\gamma(r)$, causes a vertical loading proportional to the curvature ∇^2w , much as a liquid’s surface tension causes a capillary pressure. We therefore have

$$\frac{1}{r} \frac{d}{dr} \left(\psi \frac{dw}{dr} \right) = p(r) - \gamma(r)\nabla^2w, \quad (6)$$

where $p(r)$ is the loading of the membrane caused by the pressure within the liquid.

Equations (5) and (6) can be applied to the two regions $r > R$ and $r < R$ separately, before determining the stress throughout the membrane by matching the two solutions together at the contact line $r = R$. The two regions differ because the appropriate surface energy in each region differs: within the drop ($r < R$) there are two solid–liquid interfaces while outside the drop ($r > R$) there is one solid–vapour interface and one solid–liquid interface. This difference is accounted for by the choice of $\gamma(r)$ given in (2).

III.1. Outside the drop

Outside the drop, the only loading $p(r)$ felt by the membrane is due to the hydrostatic pressure in the liquid, ρgw . However, the drops used experimentally are typically small enough that this pressure is insignificant in comparison to the effect of surface tension. (In particular, the Bond number of the drop $Bo = \rho g R^2 / \gamma_{lv} \ll 1$.) We must therefore solve (6) with $p(r) = 0$.

With this simplification, equation (6) can be integrated once. Far from the drop we expect that the sheet should tend back to being flat, i.e. $w \rightarrow 0$ as $r \rightarrow \infty$. However, we also require that in this region $\sigma_{rr} \rightarrow \gamma'_{lv}$ where, for generality, we allow $\gamma'_{lv} \neq \gamma_{lv}$. (Elsewhere in this issue²², Huang *et al.* report experiments in which such a difference was achieved by using surfactants in the liquid bath but not in the drop.) We must therefore have $\psi \rightarrow \gamma'_{lv}r$ as $r \rightarrow \infty$. For this behaviour of ψ to be compatible with the requirement that $w \rightarrow 0$ we find that, in fact, $w = 0$ throughout the region $r > R$. Substituting $w = 0$ into (5) we find that

$$\psi = T^s r + C \gamma'_{lv} \frac{R^2}{r}, \quad (7)$$

where $T^s \equiv \gamma'_{lv} - (\gamma'_{sl} + \gamma_{sv})$. The form of this stress function ψ is often named for Timoshenko though it seems also to have been known to Lamé²¹. We also note that the solution (7) has one unknown parameter, C , which we will determine by matching this solution onto that within the drop.

III.2. Within the drop

Having solved equations (6)–(5) outside the drop, we now consider the interior of the drop, $r < R$. Here, we assume that the loading on the membrane $p(r)$ is due solely to the constant capillary pressure within the drop, i.e. $p = 2\gamma_{lv} \sin \theta_0 / R$. (Again, we are able to neglect the effects of gravity since the drop is small.) Equation (6) may then be integrated once to give

$$\frac{dw}{dr} = \frac{\gamma_{lv} R \sin \theta_0}{\psi + 2\gamma_{sl} r} \frac{r^2}{R^2}, \quad (8)$$

where the constant of integration has been set equal to zero to ensure that $w'(0) = 0$. We may then use (8) to eliminate w from (5) and obtain a differential equation for ψ . However, to simplify this calculation we introduce the change of variables suggested in a related problem¹⁷: $\phi = (\psi r + 2\gamma_{sl} r^2) / \gamma'_{lv} R^2$ and $\eta = r^2 / R^2$. This gives

$$\frac{d^2\phi}{d\eta^2} = -\frac{\alpha \eta^2}{8 \phi^2}, \quad (9)$$

where

$$\alpha = \frac{Eh \sin^2 \theta_0}{\gamma_{lv}} \left(\frac{\gamma_{lv}}{\gamma'_{lv}} \right)^3 \quad (10)$$

is a non-dimensional parameter that incorporates the mechanical properties of the system.

We require two boundary conditions to solve (9) since it is a differential equation of second order. The first of these boundary conditions arises from the requirement that the radial stress σ_{rr} should remain finite as $r \rightarrow 0$; we therefore have that

$$\phi(0) = 0. \quad (11)$$

To find a second boundary condition and hence make progress, we must consider how the solutions for $r < R$ and $r > R$ match up at the contact line, $r = R$.

III.3. The contact line

We begin by considering the two force balances at the contact line: the horizontal and vertical balances. (Shanahan⁵ showed that these simple physical ideas are recovered from more detailed energy arguments.) These force balances are obtained by resolving the various forces shown in figure 2 (including the ‘surface tensions’ for the solid interfaces) into vertical and horizontal components. We recall that the validity of membrane theory requires small gradients in the displacement w and so, for consistency, we make use of this assumption in writing these force balances mathematically.

Considering the vertical force balance at the contact line we have

$$(2\gamma_{sl} + \sigma_{rr}) \left. \frac{dw}{dr} \right|_{R^-} = \gamma_{lv} \sin \theta_0 \quad (12)$$

where evaluating a function at $r = R^\pm$ denotes the limit of that function as $r \rightarrow R$ from above or below. However, we note from (8) that this condition is automatically satisfied. We thus turn now to the horizontal force balance, which gives

$$(\sigma_{rr} + \gamma_{sl} + \gamma_{sv})|_{R^+} - (\sigma_{rr} + 2\gamma_{sl})|_{R^-} = \gamma_{lv} \cos \theta_0. \quad (13)$$

This equation can be rewritten as

$$[\psi]_{R^-}^{R^+} = \gamma_{lv} R (\cos \theta_0 - \cos \theta_e) \quad (14)$$

where $\cos \theta_e = (\gamma_{sv} - \gamma_{sl})/\gamma_{lv}$ is the equilibrium contact angle of the liquid on a rigid solid with the same surface properties. However, integrating the compatibility relation (5) over the interval $(R - \epsilon, R + \epsilon)$ shows that the discontinuity of dw/dr at $r = R$ does not cause a discontinuity in $(r\psi)'$. Together with the continuity of radial displacement, this shows that both ψ and $d\psi/dr$ must be continuous at $r = R$. Using (14), we therefore find that $\theta_0 = \theta_e$.

Substituting the expressions for ψ from (7) and the function $\phi(\eta)$ into equations expressing the continuity of ψ and $d\psi/dr$ we find that

$$C = \phi(1) - 1 + \frac{\gamma_{lv}}{\gamma'_{lv}} \cos \theta_e, \quad (15)$$

and

$$\left. \frac{d\phi}{d\eta} \right|_{\eta=1} = 1 - \frac{\gamma_{lv}}{\gamma'_{lv}} \cos \theta_e. \quad (16)$$

Here (16) is the missing boundary condition allowing us to solve (9) for $\phi(\eta)$. This solution may then be used to determine C (and hence the stress field outside the drop) by using (15).

IV. RESULTS

The analysis in the last section has yielded the equations and boundary conditions necessary to find the stress function ψ throughout the membrane. Within the drop, $r < R$, it is necessary to solve the differential equation (9) with boundary conditions (11) and (16). This solution must be obtained numerically, using, for example, the MATLAB routine `bvp4c`. Once obtained, $\phi(1)$ may be calculated and the value of C in (7) determined using (15).

The quantities of primary interest here are the stresses within the membrane. However, the form of the membrane equations (6) and (5) suggests that the relevant physical quantities are the effective stresses $\Sigma = \sigma + \gamma(r)$. Alternatively, we may think of the membrane as being prestressed by the presence of the interfacial energies γ_{sl} and γ_{sv} . It is then natural to incorporate this prestress into the additional stress induced by the deformation of the membrane.

In figure 3 we plot the effective stresses Σ_{rr} and $\Sigma_{\theta\theta}$ throughout the membrane for parameter values typical of previous experiments¹². This shows that while $\Sigma_{rr} > 0$, the azimuthal stress $\Sigma_{\theta\theta} < 0$ in the vicinity of the drop. This region of negative azimuthal stress is significant because it corresponds to an azimuthal compression (once the prestress from the interfacial energy has been accounted for). We therefore identify the values of r for which $\Sigma_{\theta\theta} < 0$ with the region in which wrinkling occurs.

To test the applicability of our theoretical model to the understanding of previous experiments we consider now how the size of the wrinkled region depends on the material properties of the system. To simplify matters, we shall henceforth set $\theta_e = \pi/2$ as is observed experimentally. From (7) and (15) we see that if wrinkling occurs wherever $\Sigma_{\theta\theta} < 0$ then the wrinkle length is given by

$$\frac{L_w}{R} = [\phi(1) - 1]^{1/2} - 1. \quad (17)$$

We observe that when $\theta_e = \pi/2$ the only parameter remaining in the problem is α , which was defined in (10). In particular, this means that experiments in which no surfactant was used but the membrane thickness was varied¹² may be compared to recent experiments, reported in this issue²², in which various amounts of surfactant were used to lower the surface tension of

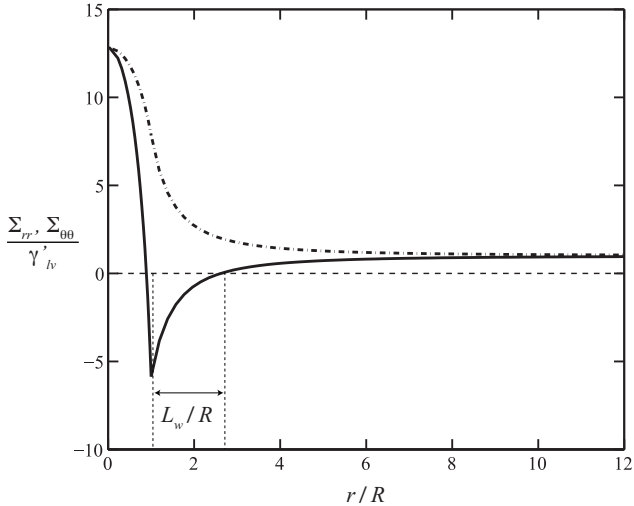


FIG. 3. Effective stress profiles within the membrane for $\alpha = 10^4$, $\theta_e = \pi/2$. Note that the radial stress Σ_{rr} (dash-dotted curve) is positive everywhere while the azimuthal stress $\Sigma_{\theta\theta}$ (solid curve) is negative for some values of r . The region outside the drop for which $\Sigma_{\theta\theta} < 0$ is highlighted by the two vertical dashed lines; the length of the wrinkles L_w is the extent of this region. In the model developed here, $\Sigma_{\theta\theta}$ and Σ_{rr} depend on γ_{sl} and γ_{sv} only through the equilibrium contact angle, θ_e .

the liquid bath but the membrane thickness held constant. This comparison is shown in figure 4 along with the empirical fit (1) proposed previously¹² and the theoretical prediction based on (17). We also note that the two solid surface energies, γ_{sv} and γ_{sl} , do not enter into the problem except via the combination $\gamma_{sv} - \gamma_{sl}$, which may be eliminated in favour of $\gamma_{lv} \cos \theta_e$. We expect that the values of γ_{sv} and γ_{sl} will not be altered by the addition of surfactant (because the surfactant will adsorb preferentially to the liquid–vapour interface) and so the equilibrium contact angle remains $\theta_e = \pi/2$.

We draw two conclusions from the comparison between experimental and theoretical results presented in figure 4. Firstly, experiments with surfactant and experiments without surfactant appear to collapse onto a single master curve parametrized by α . This lends support to the model developed here because the parameter α is a result of the theoretical analysis. Secondly, we see that the order of magnitude of the predicted L_w is in agreement with that observed experimentally, even though this prediction is consistently below the experimental value. We shall discuss the likely reasons for this discrepancy in the next section.

V. CONCLUSIONS

In this article we have presented a simple, physical model to explain the observation of a finite penetration

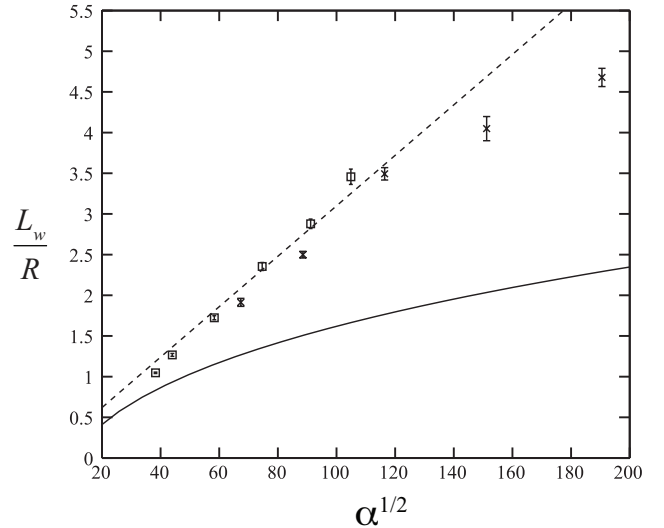


FIG. 4. Experimental results for the measured wrinkle length in experiments with surfactant²² (crosses) and without surfactant¹² (squares) as a function of the parameter α , defined in (10). The dashed line gives the empirical relationship (1), which was obtained previously¹² by fitting experimental data obtained in the absence of surfactant $\gamma'_{lv} = \gamma_{lv}$. The results of the model presented here is shown by the solid curve.

length of wrinkles observed in earlier experiments¹². This model has shown that it is vital to incorporate the surface energies into the equations of membrane theory. Furthermore, the membrane theory that results shows that a difference in liquid–vapour surface energy between the liquid bath and drop²² has a similar effect to changing the material properties of the membrane (namely E and h). In particular, we were able to collapse the results of two sets of experiments (one with varying thickness, h , the other with varying surface energy ratio γ'_{lv}/γ_{lv}) by using the single parameter α defined in equation (10). This collapse also extends the parameter range covered in previous experiments¹² and demonstrates that the empirical law (1) is only valid at small α . Our model also predicts that the value of the surface energies γ_{sv} and γ_{sl} are not individually important, though the equilibrium contact angle, θ_e , is.

However, we have also shown that the simple criterion that wrinkling occurs wherever $\Sigma_{\theta\theta} < 0$ is not able to produce an accurate quantitative prediction for the length of the wrinkles, L_w . This is because the presence of wrinkles alters the stress field within the membrane: the wrinkling observed here is far from threshold. From previous, related studies²³, we expect that the effect of the wrinkles will persist some distance into the otherwise unwrinkled part of the membrane. This should be expected to increase the length of the wrinkles and so the calculation presented here only gives a lower bound for the length of the wrinkles. This is in agreement with

what is found from the comparison of experiment and theory. We shall study elsewhere how the presence of wrinkles modifies the calculation.

ACKNOWLEDGMENTS

We are grateful to T. Russell, N. Menon and J. Huang for permission to use their experimental data (presented

elsewhere in this issue²²) in figure 4. We are also grateful to B. Davidovitch for many discussions. D.V. is supported by an Oppenheimer Early Career Fellowship. E.C. and M.A.B. acknowledge the support of CNRS-Conicyt 2008. E.C. thanks Fondecyt project 1095112 and Anillo Act 95.

-
- ¹ T. Young, *Phil. Trans. R. Soc. Lond.* **95**, 65 (1805).
² L. Mahadevan, M. Adda-Bedia, and Y. Pomeau, *J. Fluid Mech.* **451**, 411 (2002).
³ G. R. Lester, *J. Colloid Sci.* **16**, 315 (1961).
⁴ M. A. Fortes, *J. Colloid Interf. Sci.* **100**, 17 (1984).
⁵ M. E. R. Shanahan, *J. Adhesion* **18**, 247 (1985).
⁶ C. H. Mastrangelo and H. Hsu, *J. Microelectromech. Sys.* **2**, 33 (1993).
⁷ C. H. Mastrangelo and H. Hsu, *J. Microelectromech. Sys.* **2**, 44 (1993).
⁸ J. Bico, B. Roman, L. Moulin, and A. Boudaoud, *Nature* **432**, 690 (2004).
⁹ H.-M. Kwon, H.-Y. Kim, J. Puell, and L. Mahadevan, *J. Appl. Phys.* **103**, 093519 (2008).
¹⁰ A. E. Cohen and L. Mahadevan, *Proc. Natl. Acad. Sci. USA* **100**, 12141 (2003).
¹¹ E. Hamm, P. M. Reis, M. L. Blanc, B. Roman, and E. Cerda, *Nat. Mater.* **7**, 386 (2008).
¹² J. Huang, M. Juskiewicz, W. H. de Jeu, E. Cerda, T. Emrick, N. Menon, and T. P. Russell, *Science* **317**, 650 (2007).
¹³ E. Cerda, K. Ravi-Chandar, and L. Mahadevan, *Nature* **419**, 579 (2002).
¹⁴ E. Cerda and L. Mahadevan, *Phys. Rev. Lett.* **90**, 074302 (2003).
¹⁵ R. Vermorel, N. Vandenberghe, and E. Villermaux, *Proc. R. Soc. Lond. A* **465**, 823 (2009).
¹⁶ E. Cerda, *J. Biomechanics* **38**, 1598 (2005).
¹⁷ J. Chopin, D. Vella, and A. Boudaoud, *Proc. R. Soc. Lond. A* **464**, 2887 (2008).
¹⁸ D. P. Holmes and A. J. Crosby, *Phys. Rev. Lett.* (2010), submitted.
¹⁹ J.-C. Géminard, R. Bernal, and F. Melo, *Eur. Phys. J. E* **15**, 117 (2004).
²⁰ E. H. Mansfield, *The Bending and Stretching of Plates*, Cambridge University Press, 1989.
²¹ S. P. Timoshenko and J. N. Goodier, *Theory of Elasticity*, McGraw Hill, 1970.
²² J. Huang, N. Menon, and T. P. Russell, *Soft Matter* (2010), submitted.
²³ A. E. Lobkovsky and T. A. Witten, *Phys. Rev. E* **55**, 1577 (1997).